SCIENTIFIC REPORTS

OPEN

Structural elucidation of a polysaccharide from *Flammulina velutipes* and its immunomodulation activities on mouse B lymphocytes

Received: 5 June 2017
Accepted: 2 February 2018
Published online: 15 February 2018

Wen-Han Wang[1], Jing-Song Zhang[1], Ting Feng[1,2], Jing Deng[3], Chi-Chung Lin[1], Hua Fan[4], Wen-Juan Yu[5], Hai-Ying Bao[2] & Wei Jia[1]

A novel polysaccharide FVPB2 was purified from fruiting bodies of *Flammulina velutipes*. Its structure was elucidated by monosaccharide composition and methylation analyses, UV-Visible and FTIR spectroscopy as well as NMR. FVPB2 was a homogeneous heteropolysaccharide (molecular weight ~1.50×10^4 Da) containing D-galactose, D-mannose, L-fucose, and D-glucose at molar ratio of 1.9:1.2:1:2.5. *In vitro* immunomodulatory studies showed FVPB2 induced proliferation of mouse spleen lymphocytes in a dose-dependent manner. The levels of IgM and IgG, secreted by B cells, increased after FVPB2 treatment. So FVPB2 has potential to be a new important immunomodulatory nutraceutical.

For thousands of years, mushrooms have been known as an important source of nutritional diet and medicine. Extensive studies have revealed that many species of mushrooms have promising potential in improving human health and preventing diseases[1]. The search for active components and investigation of the functional mechanisms of natural products used in fungal medicine are becoming increasingly important. Polysaccharides, as one of the most important components isolated from mushrooms, have been correlated with multiple pharmacological activities, such as antioxidant, immunomodulatory, and reducing blood lipid[2]. Hitherto, about 200 active polysaccharides have been isolated from mushrooms[3–5]. All these activities are due to enhancement of the immune function of the human body.

Flammulina velutipes (Curtis) Singer (*F. velutipes*), owing to its high nutritional values and attractive taste is one of the most popular edible fungi in China and Japan. Its production and consumption ranks the fourth in the edible fungi[6,7]. Therefore, most studies have been focused on the conventional nutrient profiles of *F. velutipes*, such as amino acids, vitamins and bioactive macromolecules, and increasing production to obtain the maximum benefit. The first study of *F. velutipes* polysaccharide (FVP) was reported by Kamasuka *et al.*[8]. Since then several other polysaccharides have been isolated from *F. Velutipes* fruiting bodies[9,10]. Many reports have indicated that the bioactivities of polysaccharides can be affected by various factors including structure, molecular weight, monosaccharide compositions, even the extraction and isolation methods[11,12]. For example, a polysaccharide isolated from *F. velutipes* was proven to exert anti-inflammatory effect by decreasing $CD4^+$, $CD8^+$, ICAM-1, and MPO levels in serum and on burn injury in male Wistar rats[13]. *F. velutipes* mycorrhizae polysaccharide was isolated and activated immune function of mice T cell lymphocyte[14]. Results showed that the proportions of $CD3^+$ and

[1]National Engineering Research Center of Edible Fungi, Key Laboratory of Applied Mycological Resources and Utilization of Ministry of Agriculture, Shanghai Key Laboratory of Agricultural Genetics and Breeding. Institute of Edible Fungi, Shanghai Academy of Agricultural Sciences, Shanghai, 201403, China. [2]College of Chinese Traditional Medicine, Jilin Agricultural University, Jilin, Changchun, 130118, China. [3]Key Laboratory of Culinary Science, Sichuan Tourism University, Chengdu, 610100, China. [4]Institut für Laboratoriumsmedizin Klinische Chemie und Pathobiochemie; Campus Virchow Klinikum; Charite-Universitätsmedizin, Berlin, 13353, Germany. [5]Instrumental Analysis Center, Shanghai JiaoTong University, Shanghai, 200240, China. Wen-Han Wang and Jing-Song Zhang contributed equally to this work. Correspondence and requests for materials should be addressed to W.J. (email: jiawei0726@126.com)

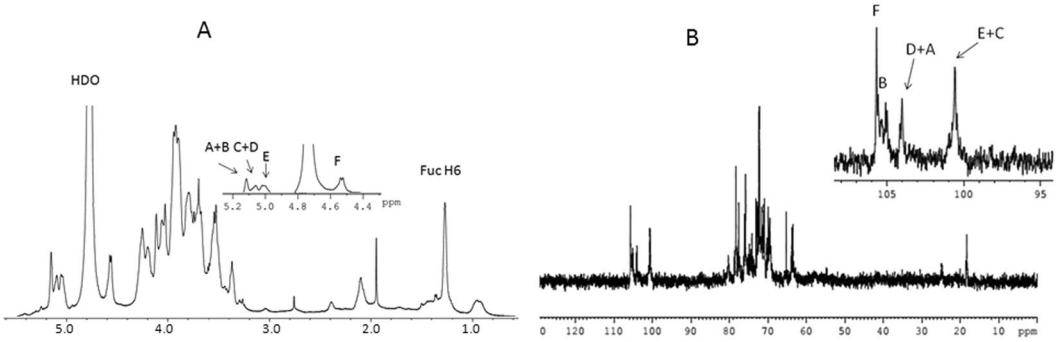

Figure 1. 500 MHz ^{1}H NMR and 125 MHz ^{13}C NMR spectrum of FVPB2 polysaccharide in deuterium oxide (D_2O) at 27 °C. The anomeric protons are labeled as (**A**–**F**). (**A**). 500 MHz ^{1}H NMR spectrum of FVPB2 polysaccharide in D_2O at 27 °C. The anomeric protons are labeled as (**A**–**F**). (**B**) 125 MHz ^{13}C NMR spectrum of FVPB2 polysaccharide in D_2O at 27 °C).

$CD4^+$ T lymphocytes; the ratio of $CD4^+/CD8^+$ and the levels of interlukin-2 (IL-2) and tumor necrosis factor-α (TNF-α) were significantly increased after being fed with polysaccharides from *F. velutipes* mycorrhizae.

Recently, many studies have revealed that *F. velutipes* polysaccharides (FVP) can stimulate the immune system[1–3,15]. However, almost all the reports verified that *F. velutipes* polysaccharides have effect on T cells. Based on this background, we attempt to test whether active polysaccharides from FVP have effect on B cell lymphocytes. The objective of this study was to elucidate the chemical structure of the novel *F. velutipes* polysaccharide FVPB2 and investigate its bioactivities on mouse B lymphocytes.

Results

Composition and structural characterization of FVPB2. The high performance size exclusion chromatography (HPSEC) profile showed that FVPB2 eluted as a single symmetrical peak, indication it was a homogeneous polysaccharide. Its molecular weight was determined to be ~1.50×10^4 Da based on the calibration graph prepared with pullulan standards. Lack of absorption at 280 nm and 260 nm in the ultraviolet-visible (UV) scanning spectrum indicated that FVPB2 did not contain protein and nucleic acid. Sugar analysis and GC-MS revealed the presence of galactose (Gal), mannose (Man), fucose (Fuc), and glucose (Glc) at a molar ratio of 1.9:1.2:1:2.5.

The FVPB2 exhibited absorption bands at 3416, 2931, 1651, and 1405 cm^{-1} on the Fourier Transform Infrared (FT-IR) spectrum. The broadly stretched intense peak at 3416 cm^{-1} was due to the hydroxyl stretching vibration of the polysaccharide. The band at 2931 cm^{-1} was due to C-H stretching vibration. The relatively strong absorption peak at 1651 cm^{-1} and the weak one at 1405 cm^{-1} also indicated the characteristic IR absorption of polysaccharides. No absorption peaks at 1730 cm^{-1} indicated that there were no uronic acids[16].

Methylation analysis of polysaccharides was performed to determine the substitution pattern of monosaccharide residues. The fully methylated products were hydrolyzed, converted into partially methylated alditol acetates (PMAAs), and analyzed by Gas Chromatography-Mass Spectrometry (GC-MS). On the basis of the GC-MS data, the polysaccharide was found to contain a branched structure with mannopyranose residue and fucopyranose residue at the terminals as well as with 3,4-di-substituted galactose, 1,2-di-substituted galactose, 1,6-di-substituted glucose, and 3,6-di-substituted glucose constituting the main chain, and a glucose residue at the other terminal.

The results of ^{1}H nuclear magnetic resonance (NMR) at 500Mz (Fig. 1A), ^{13}C NMR (125 MHz, Fig. 1B), and ^{13}C-^{1}H heteronuclear multiple quantum coherence (HMQC) analyses indicated that the repeating unit of the polysaccharide comprised six sugar residues, which were designated as A-F in the ^{1}H NMR spectrum according to the decreasing chemical shifts of the anomeric protons.

The ^{1}H NMR spectrum of FVPB2 (Fig. 1A) at 27 °C mainly contained signals for six anomeric protons at δ 4.58 to δ 5.17. One signal at 1.28 ($J_{H\text{-}5,\ H\text{-}6} = 6.42$ Hz) corresponded to the ^{1}H signal for CH_3-C group of Fuc[17]. Other signals of sugar protons were in the region of δ 4.49 to δ 3.25.

The peaks in the ^{1}H NMR spectrum (Fig. 1A), which was supported by both ^{13}C NMR (Fig. 1B) and ^{1}H -^{13}C HMQC showed six anomeric signals at δ 5.17 (single broad peak (br.s), δ 5.16 (br.s), δ 5.11 (br.s), δ 5.09 (br.s), 5.06 (br.s), and δ4.58 (double peaks (d), $J_{H\text{-}1,\ H\text{-}2} = 10$ Hz), were designated as A-F, corresponding to the signals at δ 104.02, 105.58, 100.50, 104.10, 100.59, and 105.69, respectively, in the ^{13}C NMR spectrum. Furthermore, a signal at δ 18.36 upfield revealed a CH_3-C group (C-6 of Fuc)[16].

The identities of the monosaccharide residues A-F were established based on 2D-NMR spectra analysis involving ^{1}H-^{1}H correlated spectroscopy (COSY), total correlation spectroscopy (TOCSY), nuclear overhauser effect spectroscopy (NOESY), and ^{1}H-^{13}C HMQC, which were used to assign the chemical shifts and anomeric configurations of the six sugar residues present in the repeating unit.

Residue A has an anomeric signal at δ 5.17. The proton chemical shifts from H-1 to H-6 for residue A were assigned from COSY, TOCSY and HMQC spectra (Table 1). Identification of the mannopyranose residue A signals were in accordance with the small value of $J_{H\text{-}1,\ H\text{-}2} < 3$ Hz and the large coupling constant value of $J_{H\text{-}4,\ H\text{-}5}$ (~8 Hz). The small $J_{H\text{-}1,\ H\text{-}2}$ value for the D-mannosyl residue did not provide information about the anomeric configuration[18]. The α configuration of mannose residue was inferred from the value of $J_{C\text{-}1,\ H\text{-}1} = 170$ Hz in HMBC[19].

Residue	Proton or carbon					
	H-1/C-1	H-2/C-2	H-3/C-3	H-4/C-4	H-5/C-5	H-6/C-6
A α-D-Man*p*(1 →	5.17	4.12	3.91	4.06	3.82	3.56[a], 3.70[b]
	104.02	72.73	71.48	69.48	76.19	65.21
B - →3,4)- α-D-Gal*p*(1 →	5.16	3.98	**4.04**	**4.22**	3.91	3.80[a], 3.96[b]
	105.69	73.07	**80.09**	**77.65**	71.52	63.76
C →6)-α-D-Glc*p*(1 →	5.11	3.84	3.74	3.94	4.07	**3.95[a], 3.79[b]**
	100.50	76.07	73.07	72.11	72.51	**69.50**
D α-L-Fuc*p*(1 →	5.09	3.89	4.12	3.91	4.23	1.28
	104.10	71.52	72.73	71.52	69.91	18.36
E →2)-α-D-Gal*p*-(1 →	5.06	**3.90**	4.07	3.93	4.27	3.68[a], 3.94[b]
	100.59	**80.26**	72.23	72.15	71.52	65.24
F →3,6)-β-D-Glc*p*-(1 →	4.58	3.38	**3.56**	3.69	3.91	**4.26[a], 3.92[b]**
	105.58	75.76	**78.30**	71.35	71.52	**71.52**

Table 1. ^{1}H and ^{13}C NMR chemical shifts (ppm) of FVPB2 at 27 °C. [a]Chemical shift for H-6a. [b]Chemical shift for H-6b.

Except for the downfield shift of C-1 (δ 104.02), no carbon signal was evident within the δ 76–82 range indicating that A was a terminal α-D-mannopyranose[20].

Using similar approaches, the spin system with the H-1 (B) signal at δ 5.16 was obtained from the complete proton and carbon chemical shifts (Table 1). The H-3 and H-4 signals of residue B overlapped due to similar chemical shifts. The downfield shifts of the C-3 (δ 80.09) and C-4 (δ 77.65) carbon signals with respect to the standard values for galactopyranose indicated that residue B was 1, 3, 4- α-D-Gal*p*.

The H-1 signal at high field (δ 5.11) and a small value of $J_{H\text{-}1,\,H\text{-}2} = 0$ indicated that residue C is an α-linked residue[21]. Proton chemical shifts from H-2 to H-6 were assigned from 2D NMR, including COSY, TOCSY, NOESY, HMBC and HMQC spectra. The large $J_{H\text{-}2,\,H\text{-}3}$ value and $J_{H\text{-}3,\,H\text{-}4}$ coupling constants (9 Hz) and the typical H-1, H-2, and H-4 intra-correlations in the NOESY spectrum pointed to residue C as D-glucopyranose[21]. The downfield chemical shift of the C-6 (δ 69.50) carbon signal with respect to standard values for glucopyranoses indicated that residue C is a 1,6-link α-D glucopyranose.

The anomeric signal at δ 5.09 and the small $J_{H\text{-}1,\,H\text{-}2}$ value indicated that residue D is an α-linked residue. The ^{1}H resonances for H-2, H-3, and H-4 of this residue were assigned from COSY, TOCSY, and NOESY spectra. H-5 and H-6 were assigned from the ^{1}H-^{1}H COSY spectrum. The cross-peak of H-6 and C-4 in the HMBC spectrum unambiguously showed that H-5 and H-6 were located in residue D. The proton chemical shift for the methyl group at δ 1.28 indicated an α-fucose residue. Both carbon and proton chemical shifts were typical of 6-deoxyhexopyranose, and residue D can only be L-fucose since this sugar was the only deoxyglucose identified by the GC-MS analysis. Except for the downfield shift of C-1 (δ 104.10), no carbon signal was evident within the δ 76–82 range indicating that residue D is a terminal alpha-L-Fuc*p*.

Residue E had an anomeric signal at δ 5.06 and a very small $J_{H\text{-}1,\,H\text{-}2}$ value, indicating an α-linked residue. The cross-peak δ 5.06/3.90 was detected in the COSY spectrum and, since δ 5.06 corresponded to H-1, the δ 3.90 signal was assigned to H-2. The ^{1}H resonances for H-3 were assigned from the cross-peaks in the COSY and TOCSY spectra. The H-4 and H-5 resonances were assigned from the H-3/H-4 and H-4/H-5 cross-peaks in the NOESY spectrum. The H-6a and H-6b resonances were obtained from the COSY spectrum. The large coupling constant value $J_{H\text{-}3,\,H\text{-}4}$ (~8.0 Hz) and the small coupling constant value $J_{H\text{-}4,\,H\text{-}5}$ (<3.0 Hz) suggested that residue E is a galactopyranose. The downfield shift of the C-2 (δ 80.26) carbon signal with respect to the standard value for galactopyranose indicated that residue E is (1,2)-α-D-Gal*p*.

The H-1 signal at high field (δ 4.58) and large $J_{H\text{-}1,\,H\text{-}2}$ coupling constant indicated that residue F is a β-linked residue. Proton chemical shifts from H-2 to H-6 were assigned from 2D NMR, including COSY, TOCSY, NOESY, HMBC and HMQC spectra. The large $J_{H\text{-}2,\,H\text{-}3}$ and $J_{H\text{-}3,\,H\text{-}4}$ coupling constants (9 Hz) and the typical H-1, H-2, and H-4 intra-correlations in the NOESY spectrum pointed out that residue F was D-glucopyranose[22]. The downfield shifts of the C-3 (δ 78.30) and C-6 (δ 71.52) carbon signal with respect to standard values for glucopyranoses indicated that residue F was a 1,3,6-link β-D Glc*p*.

The sequence of the glycosyl residues was determined from NOESY studies followed by confirmation by HMBC experiments. Inter-residue NOESY correlations were observed between H-1 of residue A and H-3 of residue B, between H-1 of residue B and H-6 of residue C, between H-1 of residue D and H-6 of residue F, as well as between H-1 of residue F and H-2 of residue E. Between H-3 of residue B and H-1 of residue A, Between H-4 of residue B and H-1 of residue E, Between H-6 of residue C and H-1 of residue B, Between H-2 of residue E and H-1 of residue F, Between H-6 of residue F and H-1 of residue D. HMBC experiments demonstrated clear correlations between H-4 of residue B and C-1 of residue E, between H-2 of residue E and C-1 of residue F, between H-1 of residue F and C-2 of residue E, as well as between H-3 of residue F and C-1 of residue C.

Based on the data presented above, polysaccharide FVPB2 has the following repeating unit (Fig. 2).

Effect of FVPB2 on proliferation of mouse spleen lymphocytes. Lymphocytes were prepared from the mouse spleens and treated with various concentrations of FVPB2. As shown in Fig. 3A, FVPB2 stimulated the proliferation of mouse spleen lymphocytes in a dose-dependent manner. The results also showed that

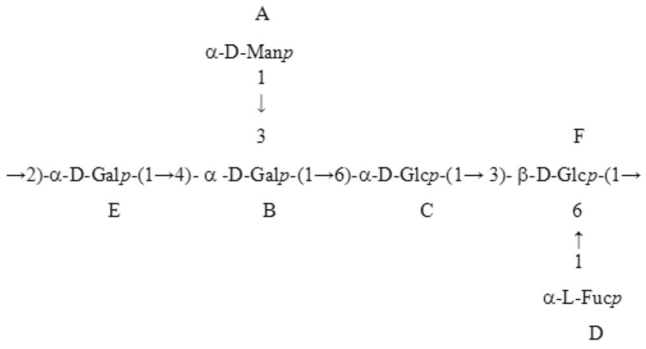

Figure 2. Repeating unit of FVPB2.

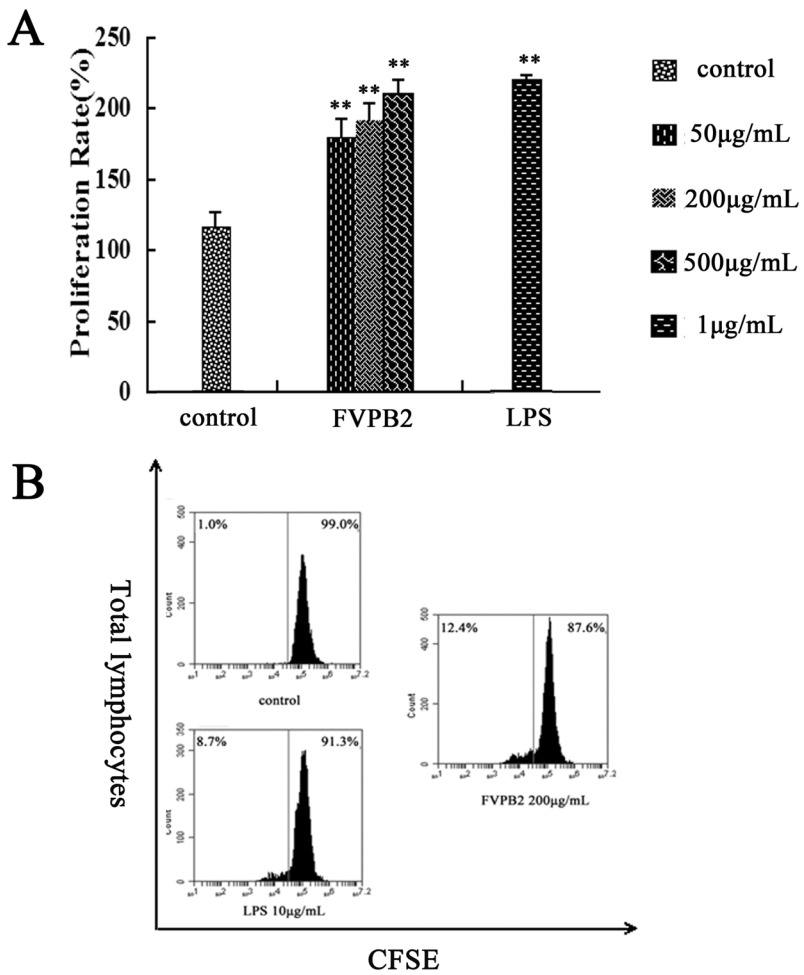

Figure 3. Proliferation of mouse spleen lymphocytes were stimulated by FVPB2. (**A**) Cells were treated by FVPB2 at the indicated concentration for 72 h (*$P < 0.05$ or **$P < 0.01$, vs. control); (**B**) After stimulation by 200 μg/mL FVPB2 for 48 hours, analysis of lymphocytes was performed by FACS. Phosphate-buffered saline (PBS) and medium containing 10 μg/mL LPS served as the negative and positive controls respectively.

proliferation rate of lymphocytes treated with 500 μg/mL FVPB2 was similar to that of lipolysaccharide (LPS) (1 μg/mL).

Carboxyfluorescein succinimidyl ester (CFSE) is an intracellular fluorescent dye that dilutes 2-fold when a cell divides[22]. Cells are typically labeled with CFSE *in vitro* and labeled cells can be followed there after *in vitro* or *in vivo*. As shown in Fig. 3B, the proliferation rates of the control and FVPB2 treated groups (200 μg/mL) were 1.03% ± 0.35% and 15.67% ± 3.00% respectively.

Our experimental results indicated that the proliferation of lymphocytes treated with 200 μg/mL FVPB2 increased by 14.64% as compared to control. Furthermore, the enhancement of cell proliferation by FVPB2 was better than that of B cells treated with LPS (13.9% vs. 4.64%).

Identification of activation of B lymphocytes treated by FVPB2. After mouse spleen lymphocytes had been stimulated by FVPB2, the mouse spleen lymphocytes were double stained either with anti-CD19-PE and anti-CD25-APC to identify the stimulated sub-population of lymphocytes. Compared with the control, the activated B cells ($CD19^+/CD25^+$) ratio increased after treatment with FVPB2 (Fig. 4A). In addition, some of the lymphocytes treated by FVBP2 enlarged by electron microscopy.

Effects of FVPB2 on levels of Immunoglobulin G (IgG) and Immunoglobulin M (IgM) antibodies secreted from B cells were examined by enzyme-linked immunosorbent assay (ELISA). Compared with the control, IgG and IgM secretion increased in mouse spleen lymphocytes treated with 200 μg/mL FVPB2 at 4, 8 and 10 days (Fig. 4B). The results indicated that the release of IgG and IgM peaked at the forth days after treatment by FVPB2, and the levels of these two immunoglobulins decreased with longer treatment time.

Effect of FVPB2 on the proliferation of B cells isolated from mouse spleen lymphocytes. To study the effect of *F. velutipes* polysaccharide on B cell proliferation, FVPB2 was used to treat the mouse spleen B cells directly, which were purified from mouse spleen-derived lymphocytes using MS Columns with anti-CD19 MicroBeads. The result of FACS showed that the percentage of B cells (CD19+/CD3−) was more than 90%. As shown in Fig. 5, the proliferation ratio of B cells treated with FVPB2 (200 μg/mL) increased more than 10.7% compared with the control group. Comparing Fig. 5 with Fig. 3B, these experiments proved that FVPB2 could promote B cells bioactivities.

Effect of FVPB2 on activation of B cells isolated from mouse spleen lymphocytes. In order to identify the activation effect of FVPB2 on B cells, the expression of CD19 and CD25 on the surfaces of purified B cells were detected. The results revealed that the percentage of activated B cells ($CD19^+CD25^+$) increased significantly after treatment with 200 μg/mL FVPB2, which are similar to the experimental results in Fig. 6A.

The proliferation and activation effects of B cells were identified in the above experiments. The secretion of IgG and IgM by B cells was analyzed by ELISA. As shown in Fig. 6B, 200 μg/mL of FVPB2 enhanced the IgG and IgM release levels at 4, 8 and 10 days.

Effect of IL-10 derived from regulatory B cells on B cells *in vitro*. To investigate the induction of FVPB2 on Interleukin 10 (IL-10) released by B cells, the expression level of IL-10 was determined by ELISA. Figure 7 shows that 200 μg/mL FVPB2 significantly enhanced the released level of IL-10 compared with control group.

The roles of extracellular regulated protein kinases (Erk1/2) and nuclear factor kappa-light-chain-enhancer of activated B cells (NF-κB) pathways on the IL-10 production by B lymphocytes cells were explored. IL-10 induction involves transcriptional activation via promoter binding of the transcription factors p38 and Activator protein 1 (AP-1)[23,24]. Purified B lymphocytes were chosen as a model to study the mechanisms. To assess whether FVPB2-induced IL-10 is dependent on ERK1/2 and NF-κB activation, purified B cells were preincubated with 5 μM ERK1/2 and 5 μM NF-κB inhibitor for 1 h respectively, followed by treatment with FVPB2 (200 μg/mL) for 3 days, and Brefeldin A, inhibitor of intracellular protein transport, was added for the last 5 h, and then the intracellular IL-10 was analyzed by FACS.

ERK1/2 inhibitor attenuated IL-10 expression in B lymphocytes cells treated with 200 μg/mL FVPB2, and IL-10 production decreased from 5.1% to 1.8%, and the inhibitory ratio of IL-10 production was 64.71% (Fig. 8). As shown in Fig. 8, NF-κB inhibitor attenuated IL-10 expression in B lymphocty cells administrated with 200 μg/mL FVPB2, and IL-10 production decreased from 5.1% to 1.0%, and the inhibitory ratio of IL-10 production was 80.39%.

Discussion

In this study, we have shown that FVPB2 with the molecular weights of ~1.50×10^4 Da was separated using hot-water extract and isolated by DEAE-Sepharose Fast Flow (26 mm × 100 cm) and Sephacryl™ S-300 gel chromatography (16 mm × 100 cm). Sugar analysis, methylation analysis, and 1D and 2D NMR spectroscopy revealed that FVPB2 was a new polysaccharide. Although several polysaccharide structures from *F. Veultipes* have been reported recently, the polysaccharide moiety of FVPB2 represents a previously undocumented novel structure[25–27]. Research is ongoing in our laboratory to further characterize the nature of the polysaccharide and to investigate structure-activity relationships.

We found the crude polysaccharide from *F. Veultipes* had anti-infamamtory effect, however, others reported the crude polysaccharides from *F. Veultipes* had pro-inflammatory effects. As it is known, the determination of the composition of crude polysaccharides are complicated, and many reports indicated that 3D-structure of a polysaccharide was closely related to biological activity[28,29], consequently, the purified polysaccharide rather than crude polysaccharide should be used for biological activity research. Yan *et al.* reported a novel polysaccharide from *F. Veultipes* (MW ~ 140 kD) consisted of mannose, glucose, galactose, fucose and rhamnose in a molar ratio of 2:4:5:1:1, and could be bound to peritoneal macrophages and strongly stimulate them to produce NO *in vitro*[30]. Leung *et al.* reported polysaccharide (MW ~ 200 kD) was mainly composed of β-(1 → 3)-D-linked glucose, and could trigger proliferation of splenic lymphocytes[31]. Wang *et al.* reported two purified polysaccharides FVP-1 and FVP-2 (Crude polysaccharide (FVP) was isolated by hot water extraction, protein removal, pigments elimination and ethanol precipitation from *F. Veultipes*. FVP-1 and FVP-2 were obtained by DEAE ion-exchange chromatography and SephadexG-100 gel column chromatography from FVP.) were from *F. Veultipes* mycelium, which molecular weight were 1.48×10^4 Da and 2.73×10^4 Da, respectively[32]. FVP-1 and FVP-2 could stimulate

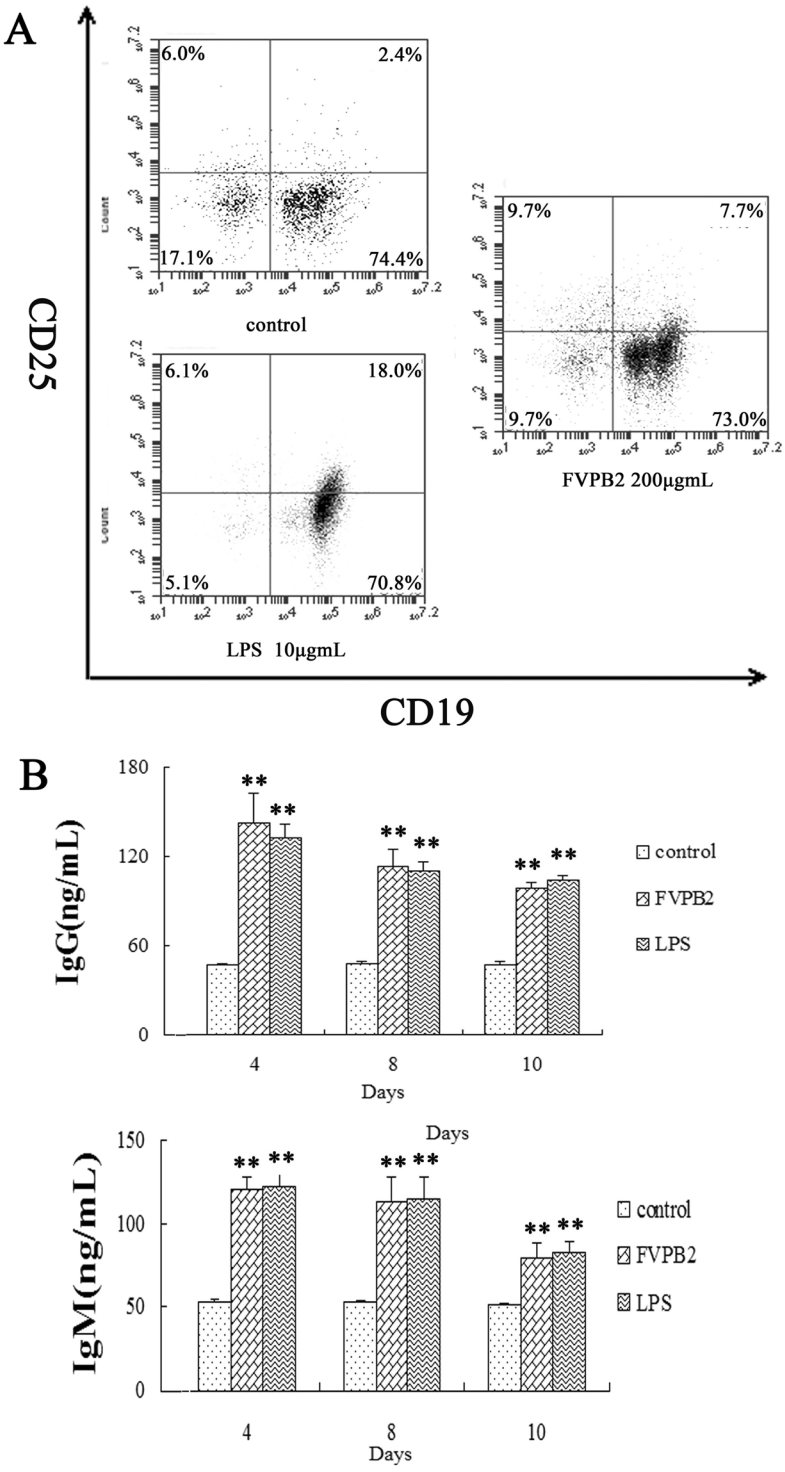

Figure 4. Identification of activation of B lymphocytes treated by FVPB2. (**A**) The activated B lymphocytes were identified with anti-CD19-PE and anti-CD25-APC. (**B**) Secretion of IgG and IgM by mouse spleen lymphocytes incubated with FVPB2. Mouse spleen lymphocytes were incubated with 200 μg/mL FVPB2, 10 μg/mL LPS or PBS. Each value represents the mean ± SD of separate triplicate experiments. Values were significantly higher than those of controls are indicated by $^{*}P < 0.05$ and $^{**}P < 0.01$).

proliferation of splenic lymphocytes *in vitro*[32]. Zhao *et al*. found that the combination of Zn and purified polysaccharide could change the immunoactivity of this polysaccharide, and exhibited its anti-inflammatory effect through inhibition of inflammatory cytokines release including IL-6, TNF-α, INF-γ and NO[33]. In this study, we demonstrated that FVPB2 had a pronounced stimulatory effect on the activation and immunoglobulin

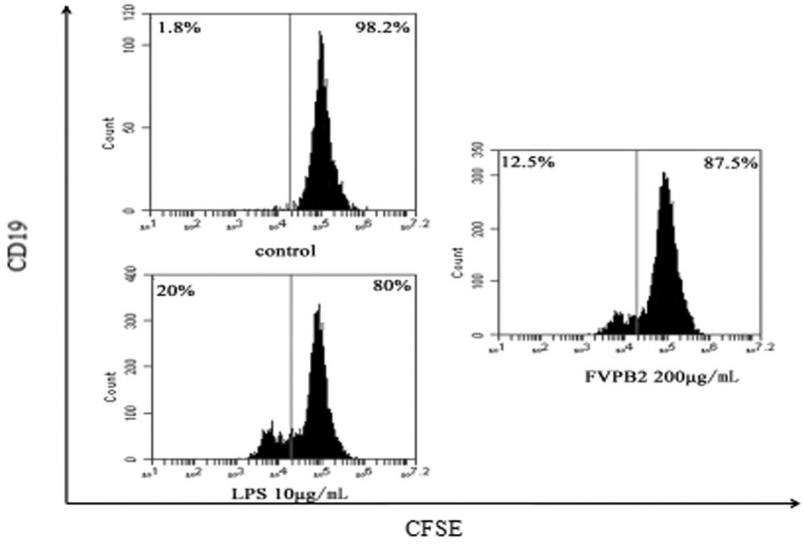

Figure 5. B cells isolated from mouse spleen-derived lymphocytes incubated with 200 μg/mL FVPB2 for 4 days. Proliferation ratio of B cells was detected by FACS. Control cells were treated with PBS.

production of B cells. B cells could regulate immune system by secreting antibodies. And T2 B cells could present antigen (they are also classified as professional antigen-presenting cells (APCs)) and secrete cytokines. Mature B cells become plasma cells which secrete antibodies such as IgG and IgM. Removal of B cells from lung lymphocyte cultures resulted in diminished IFN-β secretion and tumor lysis, providing evidence for the importance of B cell responses in tumor defenses[34]. Ollert *et al.* discovered the presence of natural IgM antibodies in the sera of healthy adults. These antibodies elicit effective killing of neuroblastoma cells by both complement activation and apoptosis[35]. These results suggested that FVPB2 have anti-tumor activity mediated by the activation and immunoglobulin production of B cells.

Regulatory B cell (Breg) is a subpopulation of B cells that play immunomodulatory role in the immune system. This unique cell population has been found to inhibit other cells in the immune system that contribute to the development of autoimmune diseases and could prove promising in the treatment of autoimmune diseases[36]. In innate cells, these mechanisms include downregulation of proinflammatory cytokine production and decreased expression of MHC-II and co-stimulatory molecules resulting in decreased T cell activation[36]. Breg can contribute to the maintenance of tolerance via the expression of immune-regulatory cytokines such as IL-10[37]. The anti-inflammatory master regulator IL-10 is a multifunctional cytokine[38]. As shown in Fig. 7 and 8, purified B cells secreted IL-10 after being treated with FVPB2. However we haven't a direct evidence for FVPB2 binding with the IL-10 receptor. As we known, IL-10 receptor 2 is a critical component of IL-10, and regulates IL-10-mediated immunomodulatory responses[39]. So whether IL-10 induction through the direct action of FVPB2 with the IL-10 receptor need to be explored in future. Some reports indicated IL-10 could regulate Ig production including IgG and IgM[40,41]. In our research, FVPB2 not only stimulated IL-10 release, but also increased IgG and IgM levels. Conceivably, these experimental results indicate FVPB2 regulated IgG and IgM expression through increasing the IL-10 level. Therefore, this new polysaccharide may possibly play an important role for the treatment of autoimmune and inflammatory diseases. To investigate the possible regulatory pathways in IL-10 expression, ERK1/2 and NF-κB inhibitors were added into the culture media of purified B cells, and IL-10 production was detected by FACS. ERK1/2 and NF-κB exist as inactive complex with class of inhibitory proteins. NF-κB, comprised of five members, ReIA (p65), Re1B, cRel, p50 and p52, is a major target and key player in inflammatory disease, which regulates various genes involved in immune and acute phase inflammatory responses[42–45]. Intracellular staining for interleukin-10 continues to be a consistent and reproducible method for identifying Breg in B cells. Figure 8 shows that ERK1/2 and NF-κB inhibitors influenced the expression of IL-10. The results clearly indicate that FVPB2 induction IL-10 is at least partially dependent on ERK1/2 and NF-κB activation in B cells.

In conclusion, our experimental results demonstrated that the new polysaccharide from *F. velutipes* (FVPB2) had typical immunostimulatory activity which was identified by promotional effects on the activation of B cells and release of IgG and IgM. In addition, our results indicate that FVPB2 had significantly upregulatory effect on IL-10 production, which has close relationship with Breg. It also indicates that this promotional effect on IL-10 production was regulated through the ERK1/2 and NF-κB signaling pathways. Accordingly, it is conceivable that the novel polysaccharide FVPB2 from *F. velutipes* has the potential to be an important new nutraceutical.

Methods

Materials and reagents. Fresh air-dried *F. velutipes* fruiting bodies were purchased from Shanghai Xuerong Bio-technology Co., Ltd (Shanghai, China). DEAE-Sepharose Fast Flow ion exchange and Sephacryl S-300 High Resolution media were purchased from GE Healthcare (Cardiff, UK). D-Gal, D-Ara, L-Fuc, L-Rha, D-Man, D-Xyl, D-Glc, D-glucuronic acid (GlcA), D-galacturonic acid (GalA), inositol and LPS (from *Escherichia coli*

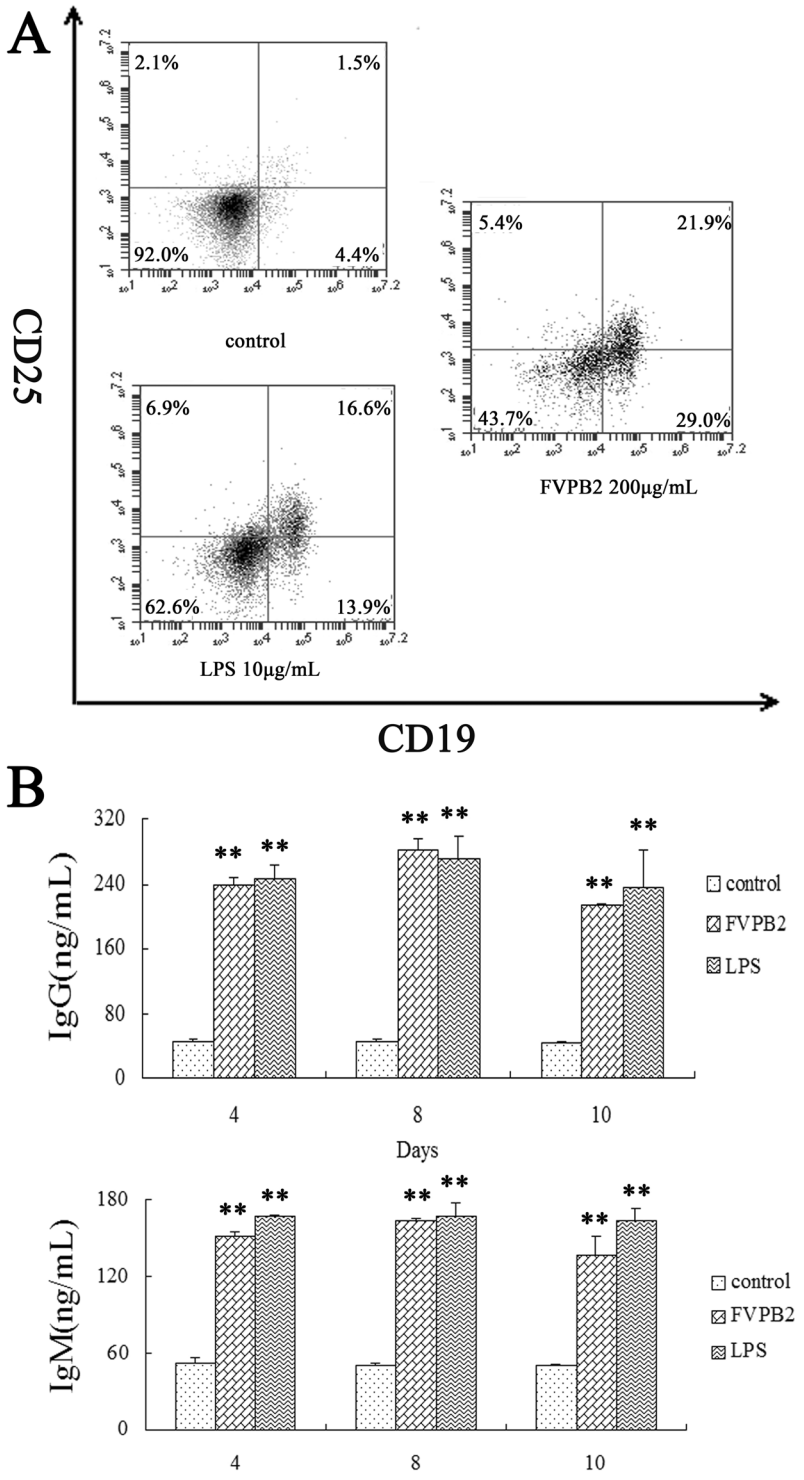

Figure 6. Activation of B cells isolated from mouse spleen lymphocytes treated by FVPB2. (**A**) Expression level of CD19 and CD25 on purified B cells, which were treated by 200 μg/mL FVPB2, 10 μg/mL LPS, or PBS for 48 h as analyzed by FACS. (**B**) Secretion of IgG and IgM by purified B cells treated with FVPB2. Purified B cells were incubated with 200 μg/mL FVPB2, 10 μg/mL LPS or PBS as control. Each value represents the mean ± SD of separate triplicate experiments. Values significantly higher than those of the controls are indicated by $*P < 0.05$ and $**P < 0.01$).

O55:B5 Sigma-Aldrich code: L2880-10MG) were all analytical reagent grade from Sigma-Aldrich (St. Louis, USA). RPMI-1640 medium and FBS was purchased from GIBCO (Grand Island, NY, USA). MS Separation Column and CD19 MicroBeads, mice were purchased from MASS Miltenyi Biotec (CA, USA). CellTrace™

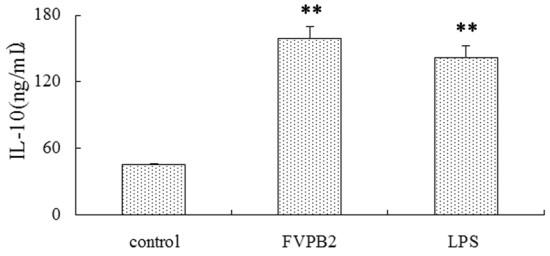

Figure 7. Effect of FVPB2 on IL-10 released by purified B cells was investigated by ELISA assay. The B cells were incubated with 200 μg/mL FVPB2, 10 μg/mL LPS or PBS (as control) for 4 days. Each bar represents the mean ± SD of three replications. Values with asterisks are significantly different (**$P < 0.01$ VS control).

5-(and 6)-Carboxyfluorescein diacetate succinimidyl ester (CFSE) Cell Proliferation Kit were purchased from Thermo Fisher (Waltham, MA). The Cytofix/cytoperm™ Fixation/Permeabilization Kit and interleukin-10 (IL-10) were purchased from BD Biosciences (CA, USA). NF-κB inhibitor (SC75741) and extracellular signal-regulated kinase 1/2 (ERK1/2) inhibitor (PD98059) were purchased from Selleck Chemicals (Houston, USA). C57 mice were purchased from Model Animal Research Center of Nanjing University (Nanjing, China). IgG, IgM and IL-10 ELISA kits were purchased from Shanghai Jake Biological Technology Co., Ltd (Shanghai, China) AlamarBlue® (#BUF012B) was from AbD Serotec (Oxford, UK). All other reagents were analytical reagent grade from Sinopharm Chemical Reagent Co., Ltd (Shanghai, China).

Extraction and purification of the FVPB2 polysaccharide. The fruiting bodies of *F. velutipes* were extracted with 95% ethanol for about 12 h to remove lipids. This step was repeated three times. After filtration, the residue was air-dried at room temperature, and then extracted with 100 °C distilled water twice (for 2 h each time). The liquid extracts were combined, centrifuged (26,000 × *g*, 20 min, 20 °C), concentrated to one-tenth of the original volume, and precipitated by adding 95% (v/v) ethanol until the final alcohol concentration reached 30%. The precipitated crude material was then washed with 95% (v/v) ethanol, resuspend in distilled water to the original volume, precipitated once more with 95% (v/v) ethanol, collected by centrifugation (26,000 × *g*, 20 min, 25 °C), and lyophilized, defined as FVP30. The FVP30 was washed with 95% (v/v) ethanol, resuspended in distilled water to its original volume, precipitated with 95% (v/v) ethanol again, and then collected by centrifugation (26,000 × *g*, 20 min, 25 °C), and then freeze dried. One gram of freeze dried material was resuspended in 100 mL of distilled water, and centrifuged as above. This solution was dialyzed (cut-off at 8.0–10 kDa) against running distilled water for 2 days, concentrated to 100 mL under reduced pressure at 40 °C and then centrifuged as before. The supernatant was applied to a DEAE-Sepharose Fast Flow column (XK26 × 100 cm), eluted first with distilled H_2O and then with a 0–2 M gradient of NaCl. The fractions were collected by an auto-collector, and the carbohydrate fraction was detected by phenol–sulfuric acid method[46]. FVP30B was obtained from the 0–2 M NaCl gradient eluate. FVPB2 (0.5 g, yield 0.59%) was purified by gel-permeation chromatography on a column of Sephacryl S-300 High Resolution (XK16 × 100 cm) from FVP30B.

Sugar analyses. Sample (2 mg) was hydrolyzed with 2 M trifluoroacetic acid (TFA) at 110 °C for 4 h according to Hardy *et al.*[47]. The monosaccharide composition was determined by high performance anion exchange chromatography (HPAEC) using a Dionex LC30 equipped with a CarboPac™ PA20 column (3 mm × 150 mm). The column was eluted with 2 mM NaOH (0.45 mL/min) followed by 0.05 to 0.2 M NaAc and the monosaccharides were monitored using a pulsed amperometric detector (Dionex). Monosaccharide components were determined using D-Gal, D-Glc, D-Ara, L-Fuc, L-Rha, D-Man, D-Xyl, D-GalA, and D-GlcA as standards.

Determination of purity and molecular weight. FVPB2 was dissolved into phosphate buffer (0.15 M $NaNO_3$ and 0.05 M NaH_2PO_4, pH 7) (2 mg/mL) to analyze the homogeneity and molecular weight by HPSEC. The system consisted of Waters 2695 HPLC system equipped with multiple detectors: refractive index detector (RI) and a UV detector for concentration determination, multiple angle laser light scattering detector (MALLS, DAWN HELEOS, Wyatt Technology, USA) for direct molecular weight determination and differential pressure viscometer (DP) for viscosity determination. The columns were TSK PWXL 6000 and 3000 gel filtration co lumns which were eluted with PB buffer at the flow rate of 0.5 mL/min. The column was calibrated using pullulan standards, P5 (6,200 Da), P10 (10,000 Da), P20 (21,700 Da), P100 (113,000 Da), P200 (200,000 Da) (Shodex, Japan). The column temperature and RI detector temperature were maintained at 35 °C.

Infrared spectroscopy. Aliquots of FVPB2 (1 mg) were made into KBr discs and analyzed in a Perkin-Elmer 599B FT-IR spectrophotometer (USA).

Methylation and GC-MS analyses. Methylation analysis of FVPB2 (2 mg) was conducted according to the method previously reported[48]. The methylated polysaccharide was then converted into partially methylated alditol acetates (PMAA) by hydrolysis, reduction with sodium borodeuteride ($NaBD_4$), and acetylation, followed by linkage analysis using a GC-MS system (Thermo Finnigan TRACE 2000/MS) equipped with a DB-5 MS column (30 m × 0.25 mm, 0.25 μm, 0.2 mm film thickness, temperature programmed from 180 to 270 °C at 20 °C/min, and held at 270 °C for 25 min[49]. The individual peaks of the PMAA and fragmentation patterns were identified by their

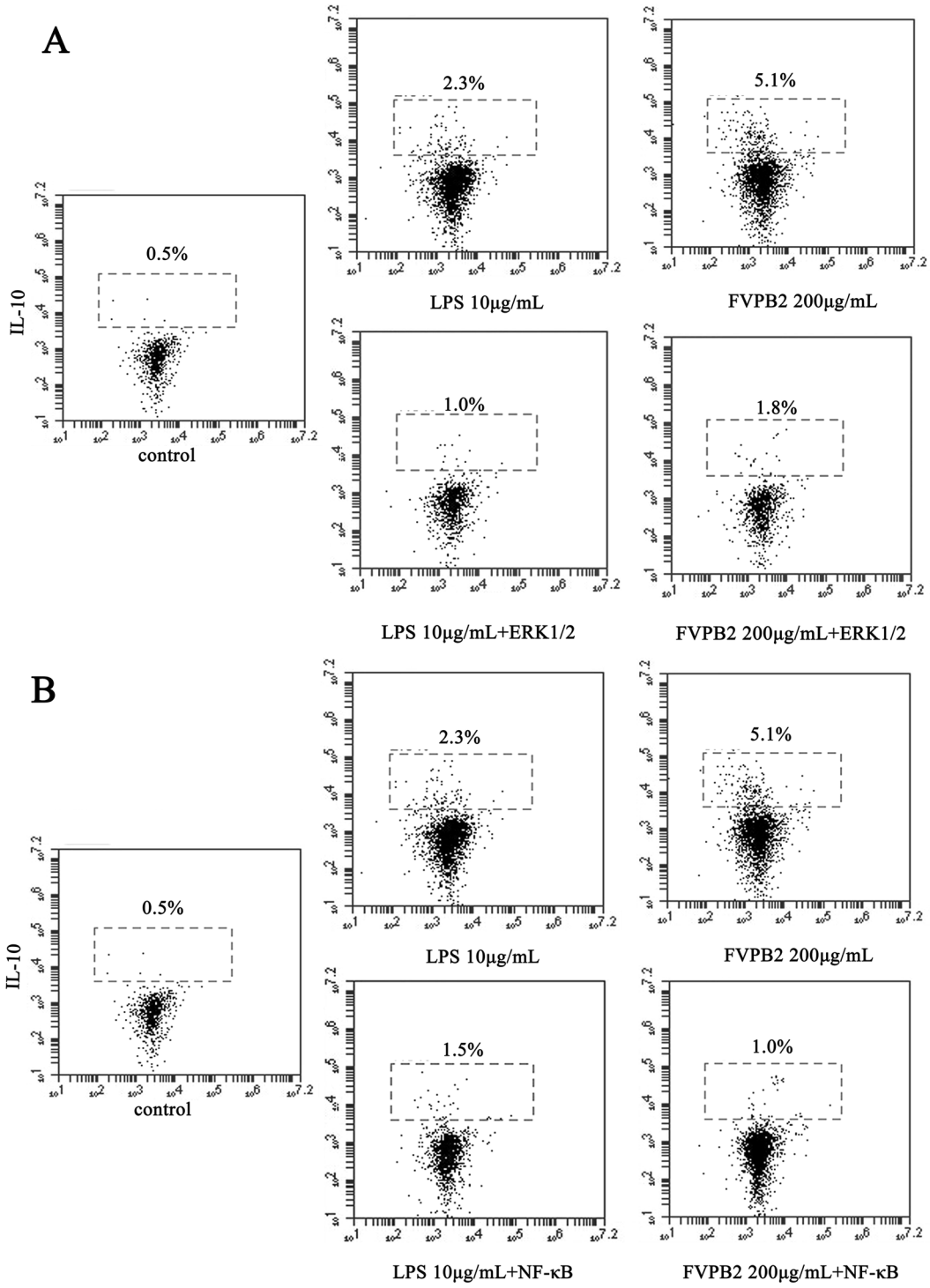

Figure 8. The influence of FVPB2 on the ERK1/2 and NF-κB signaling pathways. B cells were preincubated with 50 μg/mL ERK1/2 or 50 μg/mL NF-κB inhibitor for 1 h respectively, followed by treatment with 200 μg/mL FVPB2, 10 μg/mL LPS or PBS as the control for 3 days. Brefeldin A (BFA) was added for the last 5 h, and then the intracellular levels of IL-10 were analyzed by FACS.

mass spectra and relative retention time in NIST 2011 database of GC-MS. The percentage of methylated sugars was estimated as ratios of the peak areas.

NMR analysis. Prior to the measurements, samples were deuterium exchanged three times by freeze drying from D_2O. ^{1}HNMR (500 MHz, 27 °C) and ^{13}C NMR (125 MHz, 27 °C) spectra were recorded with a Varian INOVA 500 NMR spectrometer (USA). Chemical shifts are referenced to the HDO resonance (δ4.78) at 27 °C as

internal standard. The ^{1}H-^{1}H COSY, TOCSY, and (HMQC) were used to assign signals. HMBC and NOESY were used to assign inter-residue linkages and sequences.

Preparation of lymphocytes from mouse spleens. All experiments involving animals and their care were conducted in conformity with NIH guidelines (NIH Pub. No. 85-23, revised 1996) and were approved by Animal Care and Use Committee of the Shanghai Academy of Agricultural Sciences, Shanghai China. All experiments with animal cell lines were performed in accordance with approved guidelines, and all experimental protocols were approved in accordance with the regulations established by the Shanghai Academy of Agricultural Sciences, Shanghai China.

C57 mice, 8–10 weeks of age (ca. 23 ± 1 g), were used for lymphocyte preparation. The animals were treated according to the Institutional Animal Care and Use Committee (IACUC) guidelines. The mice were killed by cervical dislocation. The spleens were subsequently removed and cut into several pieces, and then pressed through a stainless steel mesh (100 meshes) into a culture plate using a syringe plunger. The mesh was rinsed twice with PBS under sterile conditions. The spleen cell suspension was transferred to a new tube and precipitated for 10 min. The supernatant was pipetted into another tube and the cell clumps at the bottom of the tube were discarded. After centrifugation at $400 \times g$ for 6 min, cell pellets were washed twice with PBS. In order to lyses red cells, cell pellets were resuspended for 10 min at room temperature in 1 mL Tris-HCl-buffered NH_4C1 solution pH 7.2 [mix 9 volumes of 0.83% (w/v in water) NH_4C1 with 1 volume of Tris-HCl (2.06% w/v in water, pH 7.65), adjust to pH 7.2]. Cells were counted in a Z series Counter (Counter Electronics, Miami, USA). The cell suspension was further diluted with a five-fold excess of medium. After mixing and centrifugation, the cell pellets were finally resuspended in RPMI 1640 medium containing 10% FBS (Grand Island, NY, USA).

Determination of the proliferation of mouse lymphocytes by the AlamarBlue® Assay. Lymphocytes were adjusted to a concentration of 2×10^6 cells/mL. After incubation at 37 °C in 5% CO_2 atmosphere for 24 h, the medium was removed, and 200 μL RPMI 1640 medium containing 200 μg/mL FVPB2 were added into each well. RPMI 1640 containing 10 μg/mL LPS served as positive control. After incubation for 72 h, 20 μL AlamarBlue® was added to each well, and incubated for 6 h. When the medium color changed, the absorbance at 570 nm and 600 nm were measured using a spectrophotometric plate reader (Bio-Tek Instruments, Inc, Winooski, VT, USA). The proliferation rate was calculated according to the following formula:

$$\begin{aligned} Proliferation\ rate \ = \ & [117216_* A_{570} - 80586_* A_{600}(sample)] \\ & /[117216_* A_{570} - 80586_* A_{600}(control)] \end{aligned}$$

Determination of mouse lymphocytes proliferation by CellTrace™ CFSE Cell Proliferation Kit. CFSE fluorescent dyes were dissolved in DMSO as 5 mM stock solutions (stored at −20 °C). Lymphocytes were mixed with 1 μL of stock solution at a final concentration of 10^6 cells/mL, and incubated in the dark for 20 minutes at room temperature. Cells were washed five times with RPMI 1640 (containing 10% FBS), and adjusted to a concentration of 2×10^6 cells/mL. Fresh RPMI 1640 medium containing 200 μg/mL FVPB2 were added into each well of 96-well microplate. After incubation at 37 °C in a 5% CO_2 atmosphere for 48 h (lymphocytes) or 96 h (B cells), the cells were analyzed by FACS.

Analysis of the percentage of activated B cells in spleen lymphocytes using FACS. Lymphocyte cell suspension at a concentration of 2×10^6 cells/mL (960 μL) and 40 μL of test agents were added to 24-well plates. Fresh RPMI 1640 medium containing 200 μg/mL FVPB2 were added into each well of 24-well microplate. After incubation for 48 h, lymphocytes were centrifuged, and washed twice with PBS (containing 1% BSA), and then labeled with different mAbs in PBS (containing 1% BSA) in the dark for 30 min at room temperature. After washing twice with PBS (containing 1% BSA), cells were resuspended in 0.3 mL of PBS, and sorted using BD AccuriC6 flow cytometery(BD FACSCalibur TM, Becton Dickinson, USA). FlowJo software (TreeStar, Ashland, OR) was used to analyze the percentage of various lymphocyte subpopulations. PE-conjugated anti-mouse CD19 conjugate, APC-conjugated anti-mouse CD25 and isotype control antibodies were from BD Biosciences (CA, USA).

Separation of B cells from mouse spleen lymphocytes by magnetic cell sorting. Lymphocytes were prepared from mouse spleens, washed with PBS and supernatant removed completely, and 10^7 cells were resuspended in 500 μL of buffer (PBS containing 0.5% BSA) and centrifuged at $300 \times g$ for 10 minutes. After completely aspirating supernatant, cell pellets were suspended in 90 μL of buffer per 10^7 cells, and 10 μL of magnetic cells sorting (MACS) CD19 Microbeads were added into 10^7 cells. Cell suspension was mixed well and refrigerated at 4 °C for 15 min. Supernatant was removed completely, and cells were resuspended with buffer to a concentration of 2×10^8 cells/mL. Then the cell suspension was transferred to LS + separation column which had been washed with 5 mL PBS and placed in the MidiMACS magnet. The cell suspension was run through the column, and the effluent was collected as non-B cells. Then the column was rinsed with 3 mL of buffer three times and then removed from the magnetic separator. Finally, 5 mL of buffer was added to the reservoir of LS column and the B cells were flushed out firmly using a plunger.

Quantification measurement of IgG, IgM and IL-10 using ELISA Kits. The IgG and IgM released by the B cell lymphocytes were measured by ELISA. Lymphocytes were adjusted to a concentration of 2×10^6 cells/mL. Fresh RPMI 1640 medium containing 200 μg/mL FVPB2 were added into each well of 96-well microplate. RPMI 1640 containing 10 μg/mL LPS served as positive control. Incubating at 37 °C in a 5% CO_2 atmosphere for

4 days, 8 days and 10 days, supernatant of each sample was measured using IgG and IgM ELISA kits according to the manufacturer's instructions.

The IL-10 production released by the B cells was measured by ELISA. B cells were adjusted to a concentration of 2×10^6 cells/mL. To each well of a 96-well microplate 180 μL of cell suspension and 20 μL of test agent were added. After incubation at 37 °C in a 5% CO_2 atmosphere for 4 days, supernatant was measured using IL-10 ELISA kit according to the manufacturer's instructions.

Effect of ERK1/2 (5 μM) and NF-κB (5 μM) inhibitors on IL-10 released from regulatory B cells detected by FACS. Intracellular IL-10 analysis by FACS was performed as described previously[50]. Purified mouse spleen B cells were adjusted to a concentration of 5×10^5 cells/mL. Cells (180 μL) were preincubated with ERK1/2 inhibitor (5 μM) or NF-κB inhibitor (5 μM) for 1 h. Fresh RPMI 1640 medium containing 200 μg/mL FVPB2 were added into each well of 96-well microplate, and then incubated at 37 °C in a 5% CO_2 atmosphere for 3 days. BFA was added for the last 5 h. Cells were blocked with anti-CD16/CD32 Fc-Block (Affymetrix eBioscience), fixed and permeabilized using the Cytofix/Cytoperm kit (BD Biosciences), and stained with anti-mouse PE-conjugated IL-10 (APC) mAb (BD Biosciences).

Statistical analysis. All experiments were carried out in triplicate and data were presented as mean ± standard deviation (SD). Intergroup comparisons were performed by one-way analysis of variance (ANOVA) and LSD's test. All of the variables were tested for normal and homogeneous variance by Levene's test. When necessary, Tamhane's T2 test was performed. A P value of less than 0.05 or 0.01 is significant and very significant, respectively.

Informed Consent. All experiments involving animals and their care were conducted in conformity with NIH guidelines (NIH Pub. No. 85-23, revised 1996) and were approved by Animal Care and Use Committee of the Shanghai Academy of Agricultural Sciences, Shanghai China.

References

1. Manila, P., Suonpaa, K. & Piironen, V. Functional properties of edible mushrooms. *Nutrition* **16**, 694–696 (2000).
2. Leung, N. Y., Fung, K. P. & Chay, Y. M. The isolation and characterization of an immunomodulatory and anti-tumor polysaccharide preparation from Flammulina velutipes. *Immunopharmacology* **35**, 255–263 (1997).
3. Wasser, S. P. & Weis, A. L. Therapeutic effects of substances occurring in higher Basidiomycetes mushrooms: a modern perspective. *Crit. Rev. Immunol.* **19**, 65–96 (1999).
4. Wang, H. X., Ng, T. B., Ooi, V. E., Liu, W. K. & Chang, S. T. A polysaccharide-peptide complex from cultured mycelia of the mushroom Tricholoma mongolicum with immunoenhancing and antitumor activities. *Biochem. Cell. Biol.* **74**, 95–100 (1996).
5. Wang, H. X., Liu, W. K., Ng, T. B., Ooi, V. E. & Chang, S. T. The immunomodulatory and antitumor activities of lectins from the mushroom Tricholoma mongolicum. *Immunopharmacology* **31**, 205–211 (1996).
6. Ko, W. C., Liu, W. C., Tsang, Y. T. C. & Hsieh, W. Kinetics of winter mushrooms (Flammulina velutipes) microstructure and quality changes during thermal processing. *J. Food Eng.* **81**, 587–598 (2007).
7. Leifa, F., Pandey, A. & Soccol, C. R. Production of *Flammulina velutipes* on coffee husk and coffee spent-ground. *Braz. Arch. Bio. Technol.* **44**, 205–212 (2001).
8. Kamasuka, T., Momoki, T. & Sakai, S. Antitumor activity of polysaccharide fractions prepared from some strains of Basidiomycetes. *Gann.* **59**, 443–45 (1968).
9. Ikekawa, T. *et al*. Studies on antitumor polysaccharides of *Flammulina velutipes*(Curt. ex Fr.) Sing. II. The structure of EA3 and further purification of EA5. *J. Pharmacobiodyn.* **5**, 576–581 (1982).
10. Ohkuma, T., Tanaka, S. & Ikekawa, T. Augmentation of host's immunity by combined cryodestruction of sarcoma 180 and administration of protein-bound polysaccharide, EA6, isolated from *Flammulina velutipes* (Curt. ex Fr.) Sing. in ICR mice. *J.Pharmacobiodyn.* **6**, 88–95 (1983).
11. Fan, J. L. *et al*. Characterization, antioxidant and hepatoprotective activities of polysaccharides from Ilex latifolia Thunb. *Carbohyd. Polym.* **101**, 990–997 (2014).
12. Qiu, H. Y. *et al*. Role of Macrophages in Early Host Resistance to Respiratory Acinetobacter baumannii Infection. *PloS One.* **7**, 1634–1634 (2012).
13. Wu, D. M. & Duan, W. Q. & LY, C.Y. Anti-inflammatory effect of the polysaccharides of Golden needle mushroom in burned rats. *Int. J. Biol. Macromol.* **46**, 100–103 (2010).
14. Zhu, Y. Z. *et al*. Suppressive effects of aluminum trichloride on the T lymphocyte immune function of rats. *Food Chem.Toxicol.* **50**, 532–535 (2012).
15. Yan, Z. F., Liu, N. X., Mao, X. X., Li, Y. & Li, C. T. Activation effects of polysaccharides of *Flammulina velutipes* Mycorrhizae on the T lymphocyte immune function. *J. Immunol. Res.* **170**, 54–62 (2014).
16. Ge, Q., Zhang, A. Q. & Sun, P. L. Structural investigation of a novel water soluble heteropolysaccharide from the fruiting bodies of Phellinus baumii Pilát. *Food Biotechnol.* **114**, 391–395 (2009).
17. Zhang, A. Q. *et al*. Structural elucidation of a novel fucogalactan that contains 3-O-methyl rhamnose isolated from the fruiting bodies of the fungus. *Hericium erinaceus. Carbohydr. Res.* **341**, 645–649 (2006).
18. Paramonov, N. *et al*. Structure analysis of the polysaccharide from the lipopolysaccharide of Porphyromonas gingivalis strain W50. *Eur. J. Biochem.* **268**, 4698–4707 (2001).
19. Jansson, P. E., Kenne, L. & Widmalm, G. Computer-assisted structural-analysis of polysaccharides with an extended version of CASPER using ^{1}H-NMR and ^{13}C-NMR data. *Carbohydr. Res.* **188**, 169–191 (1989).
20. Ye, L. B. *et al*. Structural elucidation of the polysaccharide moiety of a glycopeptide (GLPCW-II) from *Ganoderma lucidum* fruiting bodies. *Carbohydr. Res.* **343**, 746–752 (2008).
21. Rout, D., Mondal, S., Chakraborty, I., Pramanik, M. & Islam, S. S. Chemical analysis of a new (1 → 3)-, (1 → 6)-branched glucan from an edible mushroom. *Pleurotus florida. Carbohydr. Res.* **340**, 2533–2539 (2005).
22. Lyons, A. B. Analysing cell division *in vivo* and *in vitro* using flow cytometric measurement of CFSE dye dilution. *J. Immunol. Methods.* **2439**, 147–154 (2000).
23. Liu, B. S., Cao, Y., Huizinga, T. W., Hafler, D. A. & Toes, R. E. TLR-mediated STAT3 and ERK activation controls IL-10 secretion by human B cells. *Eur. J. Immunol.* **44**, 2121–2129 (2014).
24. Saraiva, M. & O'Garra, A. The regulation of IL-10 production by immune cells. *Immunology.* **10**, 170–181 (**2010**).
25. Yin, H. *et al*. Purification, characterization and immuno-modulating properties of polysaccharides isolated from *Flammulina velutipes* mycelium. *Am J Chin Med.* **38**(1), 191–204 (2010).

26. Liu, Y. *et al*. Purification, characterization and antioxidant activity of polysaccharides from *Flammulina velutipes* residue. *Carbohydr Polym.* **145**, 71–77 (2016).
27. Ma, Z. *et al*. Enzymatic and acidic degradation effect on intracellular polysaccharide of *Flammulina velutipes* SF-08. *Int J Biol Macromol.* **73**, 236–244 (2015).
28. Hu, J. F. *et al*. An *in vitro* study of the structure-activity relationships of sulfatedpolysaccharide from brown algae to its antioxidant effect. *J. Asian Nat. Prod.* **3**, 353–358 (2001).
29. Toida, T., Chaidedgumjorn, A. & Linhardt, R. J. Structure and Bioactivity of Sulfated Polysaccharides. *Trends Glycosci Glyc.* **15**, 29–46 (2010).
30. Yan, Y. S. *et al*. Structural investigation and activation of macrophages *in vitro of* a novel polysaccharide from Flammulina velutips mycelium. *J. China Pharm. Univ.* **42**, 164–168 (2011).
31. Leung, M. Y., Fung, K. P. & Choy, Y. M. The isolation and characterization of an immunomodulatory and anti-tumor polysaccharide preparation from Flammulina velutipes. *Immunopharmacology.* **35**, 255–263 (1997).
32. Wang, Y. F., Wang, M. & Yi, H. P. Purification, characterization and immune activity of polysaccharides from *Flammulina velutipes* Mycelium. *Chin J Nat Med.* **6**, 312–315 (2008).
33. Zhao, S. *et al*. Preparation, characterization, and anti-inflammatory effect of the chelate of *Flammulina velutipes* polysaccharide with Zn. *Food Agr. Immunol.* **28**, 162–177 (2017).
34. Liu, X. *et al*. Metabotropic glutamate receptor 3 is involved in B-cell-related tumor apoptosis. *Int. J. Oncol.* **49**, 1469–78 (2016).
35. Ollert, M. W. *et al*. Mechanisms of *in vivo* anti-neuroblastoma activity of human natural IgM. *Eur. J. Cancer.* **33**, 1942–1948 (1997).
36. Kalampokis, I. *et al*. Tedder, T.F. IL-10-producing regulatory B cells (BIO cells) in autoimmune disease. *Arthritis Res. Ther.* **15**(Suppl 1), 11–12 (2013).
37. Mauri, C. & Bosma, A. Immune regulatory function of B cells. *Annu. Rev. Immunol.* **30**, 221–241 (2012).
38. Rojas, J.M. *et al*. IL-10: A multifunctional cytokine in viral infections. *J. Immunol. Res*. 6104054 (2017).
39. Yoon, S. I. *et al*. Conformational changes mediate interleukin-10receptor2 (IL-10R2) binding to IL-10 and assembly of the signaling complex. *J. Biol. Chem*. **281**(46), 35088–35096 (2006).
40. Hummelshoj, L., Ryder, L. P. & Poulsen, L. K. The role of the interleukin-10 subfamily members in immunoglobulin production by human B cells. *Scand. J. Immunol.* **64**(1), 40–47 (2006).
41. Defrance, T. *et al*. Interleukin 10 and transforming growth factor beta cooperate to induce anti-CD40-activated naive human B cells to secrete immunoglobulin A. *J. Exp. Med.* **175**(3), 671–682 (1992).
42. Andonegui, G. *et al*. Endothelium-derived Toll-like receptor-4 is the key molecule in LPS-induced neutrophil sequestration into lungs. *J. Clin. Invest.* **111**, 1011–1020 (2003).
43. Gautam, R. & Jachak, S. M. Recent developments in anti-inflammatory natural products. *Med. Res. Rev.* **29**, 767–820 (2009).
44. Khan, A. Q. *et al*. Soy isoflavones (daidzein & amp; genistein) inhibit 12-O-tetradecanoylphorbol- 13- acetate (TPA)-induced cutaneous inflammation via modulation of COX-2 and NF-κB in Swiss albino mice. *Toxicology.* **302**, 266–274 (2012).
45. Roebuck, K. A. *et al*. Stimulus-specific regulation of chemokine expression involves differential activation of the redox-responsive transcription factors AP-1 and NF-κB. *J. Leukocyte. Biol.* **65**, 291–298 (1999).
46. Masuko, T. *et al*. Carbohydrate analysis by a phenol–sulfuric acid method in microplate format. *Anal. Biochem.* **339**, 69–72 (2005).
47. Hardy, M. R., Townsend, R. R. & Lee, Y. C. Monosaccharide analysis of glycoconjugates by anion exchange chromatography with pulsed amperometric detection. *Anal. Biochem.* **170**, 54–62 (1988).
48. Anumula, K. R. & Taylor, P. B. A comprehensive procedure for preparation of partially methylated alditol acetates from glycoprotein carbohydrates. *Anal. Biochem.* **203**, 101–108 (1992).
49. Albersheim, P., Nevins, D. J., English, P. D. & Karr, A. A method for analysis of sugars in plant cell wall polysaccharides by gas chromatography. *Carbohydr. Res.* **5**, 340–345 (1967).
50. Iwata, Y. *et al*. Characterization of a rare IL-10-competent B-cell subset in humans that parallels mouse regulatory B10 cells. *Blood.* **117**, 530–541 (2011).

Acknowledgements

The authors thank Ms. Wei Xia of the Shanghai Institute of Organic Chemistry, Chinese Academy of Sciences for valuable assistance in this study. This work was supported by Shanghai Agriculture Applied Technology Development Program, China (Grant 2012 No. 2–9).

Author Contributions

All authors conceived and designed the analysis. Wei Jia was regarded as corresponding author. Wen-Han Wang and Jing-Song Zhang were regarded as equivalent contribution authors. Ting Feng provided the updated database used. Wei Jia and Wen-Han Wang conducted the analysis and wrote the first draft of the paper, Wei Jia prepared Figs 1–2, and Wen-Han Wang prepared Figs 3–8. The GC-Ms part was directed by Wen-Juan Yu. The cell culture part was directed by Hua Fan, the revised version of our manuscript was contributed by Jing Deng, Chi-Chung Lin and Hai-Ying Bao. All authors contributed equally to the discussion of ideas and commented on the manuscript.

Additional Information

Competing Interests: The authors declare no competing interests.

Publisher's note: Springer Nature remains neutral with regard to jurisdictional claims in published maps and institutional affiliations.

Open Access This article is licensed under a Creative Commons Attribution 4.0 International License, which permits use, sharing, adaptation, distribution and reproduction in any medium or format, as long as you give appropriate credit to the original author(s) and the source, provide a link to the Creative Commons license, and indicate if changes were made. The images or other third party material in this article are included in the article's Creative Commons license, unless indicated otherwise in a credit line to the material. If material is not included in the article's Creative Commons license and your intended use is not permitted by statutory regulation or exceeds the permitted use, you will need to obtain permission directly from the copyright holder. To view a copy of this license, visit http://creativecommons.org/licenses/by/4.0/.

© The Author(s) 2018